Egyptian Journal of Veterinary Sciences

https://ejvs.journals.ekb.eg/

Pathological Alterations in Lung and Liver of Male Mice Intoxicated with Benzo[a]pyrene: A time Dependent Study

Doaa Ahmed Hassan Zedan[1], Fatma Mahmoud Darwish[1] and Iman Baker Mohamed[2]

[1]*Pathology Department, Animal Health Research Institute (AHRI), Dokki, Giza, Egypt.*
[2]*Pathology Department, Faculty of Veterinary Medicine Cairo University Giza, Egypt.*

Abstract

THIS STUDT AIMED to investigate the pathological changes occurring in lungs and liver of male mice exposed to different doses of Benzo[a]pyrene (B[a]P) over varying durations. B[a]P is a potent carcinogenic polycyclic aromatic hydrocarbon commonly found in the environment, primarily adsorbed to particulate matter. Ninety mature mice were divided into three groups: a control negative group, a group injected with a single dose of 50 mg/kg bw of B[a] P, and a group injected with a single dose of 100 mg/kg bw of B[a] P. The experiment was conducted over several months, with ten mice from each group being sacrificed at 3, 6, and 9 months. Serum samples were collected for biochemical tests to assess liver function and tumor marker alpha-fetoprotein levels. Additionally, postmortem examinations were performed; lung and liver tissue specimens were collected for histopathological analysis. The results of the biochemical tests revealed a significant increase in Alanine aminotransferase (ALT), Aspartate aminotransferase (AST) and alpha-fetoprotein levels. Histopathological examination of the lung tissues showed a gradual initiation of mild hyperplastic proliferation in the bronchiolar epithelia at both half (50 mg/kg bw) and full (100 mg/kg bw) doses of B[a] P, with more pronounced changes observed in the full-dose groups at 6 and 9 months. At 9 months of full-dose treatment, a well-defined circumscribed tumor mass was detected. In the liver, cellular changes were observed at 3 months for both half and full doses of B[a]P, progressing to malignant changes at 6 months and ultimately leading to the development of hepatocellular adenocarcinoma at 9 months.

Keywords: Benzo[a]pyrene, lung, liver, histopathology.

Introduction

Benzo [a] pyrene (B[a] P) is a five-ring polycyclic aromatic hydrocarbon (PAH) that has gained considerable attention due to it is ubiquitous in the environment with potent carcinogenic properties. It is a well-known environmental pollutant found in various sources, including combustion processes, industrial emissions, and tobacco smoke [1].B[a] P is primarily adsorbed to particulate matter in the environment, and it's widespread in air, soil, water, and food [2].

The carcinogenicity of B[a] P has been extensively studied and established. It is metabolically activated by cytochrome P450 enzymes, forming reactive intermediate metabolites that can bind to DNA, leading to the formation of DNA adducts [1, 3]. These adducts can induce genetic mutations and disrupt normal cellular processes, ultimately contributing to the development of cancer [4].

Numerous epidemiological and experimental studies have provided evidence for the carcinogenic potential of B[a] P [5].Occupational exposure to B[a] P has been associated with increased risks cancers, such as lung cancer in exposed individuals [6].Animal studies have further confirmed the carcinogenic effects of B[a] P, demonstrating the development of tumors in various organs, including the lung [7] and liver [8].

In recent years, research efforts have focused on understanding the mechanisms underlying B[a] P-induced carcinogenesis and identifying strategies to mitigate its adverse effects. Advances in molecular biology and toxicology have facilitated the elucidation of key signaling pathways and molecular targets involved in B[a]P toxicity and carcinogenicity. Additionally, the development of novel techniques, such as high-throughput genomics and proteomics, has enabled researchers to explore the comprehensive impact of B[a] P exposure on

*Corresponding authors: Doaa A. Zedan, E-mail: doaazedan3781@gmail.com, Tel.: 01017734697
(Received 07 March 2024, accepted 12 August 2024)
DOI: 10.21608/EJVS.2024.273105.1898

cellular processes and identify potential biomarkers of exposure and early disease detection [9].

Material and Methods

Ethical approval

Ethical approval for this study was obtained from Bioethics Committee of the Biotechnology Research Centre, with approval number BEC-BTRC 10-2019

Chemicals

Benzo [a] pyrene (B[a] P) in the form of a pale-yellow solid crystal was obtained from Sigma Company (Germany). Maize oil was used as the solvent for B[a] P (Immtenan company).

Experimental animals

Ninety mature male mice, aged between 1 and 1.5 months, Their weight from 40 to 45 gm., obtained from National Cancer Institute (of Egypt) and housed in galvanized in a controlled environment for two weeks prior to the start of the study. They were provided with standard feed and had access to freshwater.

Experimental design

The mice were divided into three groups, with 30 mice in each group.Group 1 served as control negative group and received intraperitoneal (I/P) injections of maize oil only. Group 2 received a single I/P injection of B[a] P at a dosage of 50 mg/kg bw, and Group 3 received a single I/P injection of B[a] P at a dosage of 100 mg/kg bw [10].

Throughout the study, all groups were closely monitored. At three-months intervals, 10 mice from each group were euthanized. Blood samples were collected from the orbital plexus without the use of anticoagulants, and serum was separated for subsequent biochemical tests.

Postmortem examinations were conducted meticulously, and tissue specimens from the lung and liver were collected from each animal for histopathological examination.

Biochemical studies

The separated serum samples were used for estimation of Alanine aminotransferase (ALT) and Aspartate aminotransferase (AST) [11] and tumor marker α-fetoprotein [12].

Histopathological studies

Representative tissue specimens from lung and liver were selected from each euthanized mouse and fixed in 10% neutral buffered formalin solution for at least 24 hours. Tissue specimens were routinely processed, paraffin embedded, sectioned at 4-6-micron thickness then stained with Hematoxylin and Eosin, PAS stain (for glycogen), and Prussian blue stain (for detection of hemosiderin pigment) [13].

Scoring system for pathological lesions

The lesion scoring for pathological lesions were done [14].Five random optical areas were checked and figured then mean of the five fields was recorded[14].Mean for 3 tissues ±standard error (SEM) was detected. Normal histological structure was given grade 0 in all organs.

Statistical analysis

The obtained data were analyzed by using SPSS 14. [15].

Results

Biochemical parameters

The impact of intraperitoneal (I/P) injection of B[a] P on various biochemical parameters in mice is summarized in Tables 1, 2, and 3. The activities of Aspartate Aminotransferase (AST) and Alanine Aminotransferase (ALT) showed a significant increase, which was both dose and time-dependent. Notably, the levels of alpha-fetoprotein were consistently elevated throughout the entire duration of the experiment, particularly in the group receiving the higher dose of B[a] P. There are significance differences ($P<0.05$) between means having different letter in the same period (month) . AST in Control no changes, while half dose showed elevation in AST by minimal changes3-6 months but the marked elevation was in 9 month. Full dose revealed the marked deviation started from 6 month to 9 month (Table 1). There are significance differences ($P<0.05$) between means having different letter in the same period (month). AlT Control showed no changes, while half dose revealed gradual elevation from 3-9 month, also in full dose marked deviation than half dose from 3-9 month (Table 2).There are significance differences ($P<0.05$) between means having different letter in the same period (month).α Feto protein in control no changes, while increased gradually in half and full dose throughout the period of experiment(Table 3).

Histopathological studies

Lung findings in mice exposed to a half-dose of B[a] P

Macroscopic findings

At 3 months, slight congestion was observed in the lungs. By the 6-month, the lungs exhibited a marbled appearance, and at 9 months, greyish whitish spots were observed on lung surface.

Microscopic findings

Lung of control animals revealed normal histological structure. (Fig. 1a)

At 3 months of treatment, the pulmonary blood vessels were widely dilated and engorged with blood; mild hyperplastic proliferation of the bronchiolar epithelium towards the bronchiolar

lumina .Emphysema in some pulmonary alveoli meanwhile others were atlectatic airless alveoli.Thickened interalveolar septa was also observed (Fig. 1 b). Meanwhile at 6 months of treatment, multi focal variable sized areas of hemorrhage were detected in the pulmonary parenchyma in many instances, the alveolar lumina contained cellular exudate composed principally of RBCs.There was hyperplastic proliferation of the bronchiolar epithelium. At the vicinity of some pulmonary bronchioles there were clusters of small round cells which showed vesicular nuclei with coarsely stippled chromatin (Fig. 1c).Sometimes numerous mitotic figures were evident in these cells. Perivascular edema and fragmentation of muscular layer of one of the pulmonary blood vessels were detected.

At 9 months of treatment, there was hyperplasia of the bronchiolar epithelium and form frond like projections toward the bronchiolar lumina (Fig. 1d). Sometimes the bronchiolar epithelium disrupt the basement membrane and invade the pulmonary parenchyma forming solid masses and or acinar like structure (Fig. 1e), the proliferated bronchiolar epithelium showed some criteria of malignancy represented by mild to moderate cellular atypia and nuclear pleomorphism.

In one case, the proliferated bronchiolar epithelium was detected in the lumen of the adjacent alveoli. In few instances the proliferated bronchiolar epithelium appeared to be dispersed individually in the pulmonary parenchyma and sometimes exhibiting mitotic activities moreover large macrophage and plasma cells were seen infiltrated in the pulmonary parenchyma (Fig. 1f).

Lung findings in mice exposed to the full dose of B[a] P

Macroscopic findings

At 3 months of treatment, the lungs exhibited moderate enlargement and congestion. Greyish foci were observed on the lung surface at 6 months.In one case at 9 months, a nodule was found at the periphery of a lung lobule. (Fig. 4A)

Microscopic findings

Lung of control animal showed normal histological structure.

At 3 months of treatment with the full dose, in addition to the previously mentioned changes, there were multifocal small areas of hemorrhage in the pulmonary parenchyma and thickened interalveolar septa. Focal hyperplastic proliferation of small round cells, uniform in size with coarsely stippled chromatin, was observed adjacent to one of the pulmonary blood vessels (Fig. 2b).

At 6 months of treatment, diffuse hemorrhage was observed in the pulmonary parenchyma. Focal aggregations of cells were found around the pulmonary bronchioles (peribronchiolar) or surrounding pulmonary blood vessels. Large macrophages or multinucleated syncytial giant cells containing golden yellow hemosiderin pigment were dispersed in the pulmonary tissue (Fig. 2c). The presence of hemosiderin pigment was confirmed using Prussian blue stain, which stained the pigment blue (Fig. 2d)

In the group treated for 9 months, the aforementioned changes were observed, along with a well-defined tumor mass originating primarily from the proliferated bronchiolar epithelium at the periphery of a pulmonary lobule. The tumor consisted of proliferated bronchiolar epithelium arranged in acinar patterns, irregular solid masses, and sheets (Fig.2 e,f).The proliferated cells exhibited various malignant characteristics, such as cellular and nuclear atypia, numerous mitotic figures, and an ill-defined stroma.Some tumor cells showed signs of necrosis with karyolysis of the nuclei. Moreover, solid masses of neoplastic cells infiltrated the lumen of adjacent bronchioles, the pulmonary parenchyma, at the vicinity of some pulmonary blood vessels.

Liver of mice intoxicated with half dose of B[a] P

Macroscopic findings

Liver showed mild congestion and enlargement at 3 months, meanwhile at 6 months liver was enlarged and have par boiled surface and round borders. At 9 months diffuse pin headed spots on the liver surface was detected.

Microscopic findings

Control mice showed nearly normal histological structure (Fig 3a)

At 3 months of treatment, the hepatic blood vessels were widely dilated and engorged with blood, the hepatic tissue exhibited focal zones of hepatocellular coagulation necrosis manifested by circumscribed deeply eosinophilic homogenous areas, moreover the adjacent hepatic tissue showed individual cell necrosis (Fig. 3b).There was focal aggregation of mononuclear cells, Kuppfer cell proliferation were evident in many instances.

At 6 months of treatment, there was focal hepatocellular necrosis where the necrotic foci were invaded by mononuclear cells.The majority of the hepatic cells revealed numerous mitotic figures, multiple nuclei and increased nuclear cytoplasmic ratio few hepatic cells are arranged in an adenoid pattern (Fig. 3c).

At 9 months of treatment, in addition to the previously mentioned changes there was focal perivascular aggregation of small round cells, mitotic figures were clearly detected where the mitotic index were 4-6 per high power field.Mild to moderate anisocytosis and anisokayosis were

evident.The hepatocytes were polygonal in shape, also there were foci of hepatocellular alteration represented by hypertrophied hepatocytes with extremely enlarged nuclei with multiple nucleoli (Fig. 3d). Formation of newly formed bile ductules and infiltration of mononuclear cells in the portal area (Fig. 3e).

Liver findings in mice exposed to the full dose of B[a]P

Macroscopic findings

At 6 months, the liver showed enlargement with the appearance of white spots dispersed all over its surface. In the group treated for 9 months, when the peritoneum was opened, transparent clear fluid oozed out.The liver was congested and there was foci of depression and others of elevations. (Fig. 4B)

Microscopic findings

Control mice revealed nearly normal histological structure (Fig. 5a)

At 3 months of treatment, the hepatic tissue exhibited multiple foci of hepatocellular alterations in the parenchyma. These altered foci were characterized by hypertrophied hepatocytes with enlarged nuclei and strong glycogen accumulation, which was evidenced by clearance of the cytoplasm (Fig. 5b).Glycogen accumulation was confirmed using PAS stain, which stained it scarlet red (Fig. 5c).Mitotic figures were observed in many instances.Mild cellular and/or nuclear atypia were observed in some cases.

At 6 months of treatment, there was disorganization of the hepatic cords with individualization of the hepatic cells. Acinar orientation of the hepatic cells were evident in many instances (Fig. 5d) and or orientation in small clusters of hepatocytes or syncytial like strucutres.The hepatocytes appeared hypertrophied with extremely enlarged nuclei with marginated nuclear chromatin (Fig. 5e), sometimes intracytoplasmic microvacuoles were observed in the proliferated hepatocytes(Fig. 6a).There were numerous foci of proliferated biliary epithelium appeared in the hepatic parenchyma in-between hepatocytes. In many instances centrilobular necrosis were detected in the hepatic tissue.

At 9 months of treatment, in addition to the previously mentioned changes the hepatic tissue revealed hepatocellular carcinoma which consisted of neoplastic cells which extremely large in size and containing large fat globules with peripherally located hyperchromatic nuclei (Fig. 6b) in addition to marked proliferation of biliary epithelium in between the neoplastic cells was also detected.

The neoplastic cells were oriented at different configuration trabecular in which it composed of 2 or 3 cell thickness or adenoid pattern as well as syncytial solid structures and separated by dilated hepatic sinusoids, sometimes hepatocytes coalesced and form multinucleated syncytial giant cell (Fig. 6c).Sometimes the acini appeared dilated and containing remnant of necrotic hepatocytes, the neoplastic cells were pleomorphic in shape having ill distinct boundaries the nuclei were enlarged with marked pleomorphism and hyperchromatism (Fig. 6d).

Scoring lesion

Criteria of malignancy in hepatocytes (mitotic figures, cytology, nuclear atypia) changed also according time and dose.

Discussion

Benzo[a]pyrene is a widely distributed environmental pollutant and a potent carcinogen belonging to the polycyclic aromatic hydrocarbon group. It is generated during the combustion of organic materials. In this study, we investigated the effects of B[a]P on the lung and liver tissues of male Swiss albino mice.

Our findings demonstrate that the histological and biochemical changes in the lung tissue were dose- and time-dependent following treatment with either a half or full dose of B[a]P.These changes gradually progressed in relation to the dose and duration of exposure. Our results are consistent with a previous study [16], which reported that increasing B[a] P concentration and exposure duration led to elevated DNA adduct levels.

In the mice exposed to B[a] P, whether at a half or full dose, significant changes were observed in the lung tissue. These changes included hemorrhage, thickening of the interalveolar septae, and infiltration of mononuclear cells in the pulmonary parenchyma. B[a]P induces lung toxicity and inflammation in mice [7]. One notable finding in our study was the hyperplasia and proliferation of bronchiolar epithelium, which progressed from bronchiolar hyperplasia to frond-like projections in the half-dose group and eventually to acinar formation and adenocarcinoma in the full-dose group.

The gradual progression of bronchiolar epithelial metaplasia towards cancer formation suggests a sequential series of events initiated by bronchiolar hyperplasia. This finding is consistent with the hypothesis proposed that multiple hyperplastic foci of bronchi and alveoli develop during the early phase of carcinogen exposure. Many of these foci do not progress further into adenomas, but after several months, some may develop into adenocarcinomas [17].

Furthermore, ciliated bronchiolar epithelial cells are highly sensitive to toxicants, and the high concentration of metabolizing enzymes in Clara cells makes them particularly susceptible to inhaled or ingested chemicals that require metabolic activation to become cytotoxic [18].On the other hand, expansion of the bronchiolar stem cell pool was associated with continuous proliferation of neuroepithelial bodies associated with Clara cells. This ultimately led to bronchiolar hyperplasia, and

with further progression, from hyperplasia into solid tumors [19].

Overall, our findings highlight the detrimental effects of B[a]P on lung tissue, including inflammation, hyperplasia of bronchiolar epithelium, and the potential development of adenocarcinoma.These results contribute to our understanding of the mechanisms involved in B[a] P-induced lung carcinogenesis.

The hyperplastic bronchiolar epithelial cells, particularly in mice treated with a full dose of B[a]P, invade the adjacent pulmonary tissue. A study on a mouse model of human lung cancer, suggested invasiveness as a characteristic feature [17].The invasion of neoplastic cells is associated with the release of proteolytic enzymes during local invasion [20].

In addition, B[a]P has genotoxic effects through metabolic reprogramming, resulting in decreased cell respiration and increased lactate production, leading to mitochondrial dysfunction (known as the Warburg effect) [4]. In our study, one of the most prominent lesions observed in the group exposed to a full dose of B[a]P for 9 months was the appearance of a circumscribed tumor mass. The carcinogenic process is considered a complex multifactorial process [21].

B[a] P is a potent lung carcinogen. During its metabolism, B[a] P produces intermediate metabolites called 7,8-diol 9,10-epoxides (BPDE), which are considered ultimate carcinogens that form mutagenic adducts with DNA.Reactive oxygen species and free radicals generated during B[a] P metabolism have been suggested to be involved in the initiation and progression of carcinogenesis [22].

Furthermore, B[a]P intoxication resulted in lipid peroxidation (LPO) and a decrease in antioxidant enzymes, inducing oxidative stress in the process of lung cancer formation [23].The high concentration of LPO products plays a significant role in the early stages of tumor formation [24].

Moving on to the liver, the histopathological and biochemical changes observed in the liver of mice intoxicated with B[a]P were found to be both time- and dose-dependent. The biochemical analysis, in our study, revealed a significant increase in the concentration of alanine aminotransferase (ALT) and aspartate aminotransferase (AST).The toxicity of B[a] P induce liver dys-function that mediated by liver damage and oxidative stress [8, 25].

The increased production of reactive oxygen species (ROS) is a major contributor to hepatic changes caused by B[a] P [1].The membranes are particularly susceptible to the effects of ROS, as their peroxidation of unsaturated fatty acids in biological membranes results in diminished fluidity and distortions.

The direct damage of reactive oxygen species (ROS) on plasma membranes leads to an increase in the permeability of hepatocytes and the subsequent release of enzymes into the bloodstream [26].In our study, we observed greater activities of enzymes associated with liver dysfunction, indicating damage to hepatocytes and increased membrane permeability.

Some enzymatic abnormalities are considered markers for cancer, either through the expression of fetal forms of enzymes or ectopic production of enzymes [27].Our results align with the majority of hepatocellular carcinomas overexpress alpha-fetoprotein (AFP) production [28].AFP is a glycoprotein derived from embryonic tissue, and its levels are high in fetal serum but gradually decrease after birth.In adults, hepatocytes do not normally synthesize AFP, but cancer cells can regain the ability to produce it [29].

Regarding the histopathological findings, one of the prominent lesions observed at 3 months was a focal zone of hepatocellular necrosis.The hepatotoxicity of B[a]P was attributed to apoptosis, autophagy, and pyroptosis.Autophagy is a stress response that occurs when cells resist unfavorable external stimuli [30].Another lesion observed in the 6-month group was the disorganization of hepatocytes.Excessive autophagy impairs cell morphology and function, leading to autophagic cell death [31].

The presence of glycogen vacuoles in hepatocytes is also noteworthy. B[a]P can induce liver dysfunction by increasing the appearance of vesicles containing degraded cellular material [32].Mononuclear cell infiltrations were a characteristic finding observed in all our groups, which attributed this to pyroptosis, a type of programmed cell death, depending on Caspase-1 activation [33].This leads to the release of a large number of pro-inflammatory cytokines such as IL-1B and IL-18, thereby inducing chronic inflammation.B[a]P toxicity also results in increased levels of nitric oxide (NO), which is one of the ROS and acts as a pro-inflammatory mediator and induces signaling for pyroptotic cell death [34, 35].Another mechanism for apoptosis is the induction of the aryl hydrocarbon hydrolase (AHH) enzyme system, which includes CYP1A1 and CYP1A2 [36].

The aromatic hydrocarbon receptor (AhR) plays a crucial role in regulating cell cycle and apoptosis, as well as other types of cellular damage.

At 3 months, preneoplastic lesions were observed, characterized by foci of hepatocellular alteration with enlarged nuclei and intense glycogen accumulation. These altered foci are considered precursors for hepatocellular carcinoma [37]. Nuclear enlargement and an increased nuclear-cytoplasmic ratio reflect the initiation of

carcinogenesis and are associated with changes in DNA [38].The strong glycogen accumulation in the area of hepatocellular alteration can be attributed to metabolic disturbance [39].

Chemical carcinogens have the ability to induce both benign and malignant tumors [40]. In the group exposed to a full dose of B[a] P for 9 months, the most pronounced finding was the appearance of hepatocellular carcinoma. B[a]P has been classified as a Group 1 carcinogen by the International Agency for Research on Cancer (2014). Once B[a]P enters the cell, it undergoes metabolic activation by the cytochrome P450-dependent monooxygenase system, resulting in the formation of reactive metabolites that covalently bind to DNA, forming carcinogenic intermediate metabolites [41].B[a] P metabolism induces the production of reactive oxygen species, which can damage cellular macromolecules [42].

Overall, the findings from the present study provide insights into the dose- and time-dependent effects of B[a] P on lung and liver tissues.The observed histopathological and biochemical changes support the role of B[a]P as a potent carcinogen in the development of lung and liver cancers.

Conclusion

In conclusion, benzo[a]pyrene (B[a] P) as an environmental pollutant has the potential to induce tumor formation even at low levels of exposure. Therefore, it is important to control exposure to this pollutant from both natural and anthropogenic sources, for the well-being of both animals and humans.

Conflicted interest

No Conflicted interest.

Acknowledgment

We thank everyone who contributed to the support of this research.

Funding statement

Self-funding

Author contribution

The researcher designed the research idea and prepared the practical part of the research, while conducting statistical analysis, writing, and final review of the research.

TABLE 1. Aspartate aminotransferase (Mean ± Standard deviation)

	3 Months	6 Months	9 Months
Control	10.7 ±1.5^{a}	12.3 ±2.5^{b}	14.0 ±3.6^{a}
Half dose	24.7 ±4.5^{b}	29.0 ±3.6^{b}	36.7 ±3.5^{c}
Full dose	29.0 ±3.6^{b}	36.3 ±3.2^{b}	45.0 ±3.0^{c}

TABLE 2. Alanine aminotransferase (Mean ± Standard deviation)

	3 Months	6 Months	9 Months
Control	10.7 ±4.2 ^{a}	10.0 ±3.6 ^{a}	15.3 ±1.5 ^{a}
Half dose	15.3 ±1.5 ^{ab}	18.0 ±4.0 ^{b}	21.7 ±3.5 ^{a}
Full dose	18.3 ±1.5 ^{b}	20.7 ±4.0 ^{b}	31.0 ±4.6 ^{b}

TABLE 3 α-feto protein (Mean ± Standard deviation)

	3 Months	6 Months	9 Months
Control	12.0 ±2.0 ^{a}	13.0 ±2.6 ^{a}	13.3 ±1.5 ^{a}
Half dose	24.0 ±5.3 ^{b}	43.7 ±8.1 ^{b}	60.0 ±5.0 ^{b}
Full dose	32.7 ±2.1 ^{c}	53.3 ±10.4 ^{b}	74.7 ±4.5 ^{b}

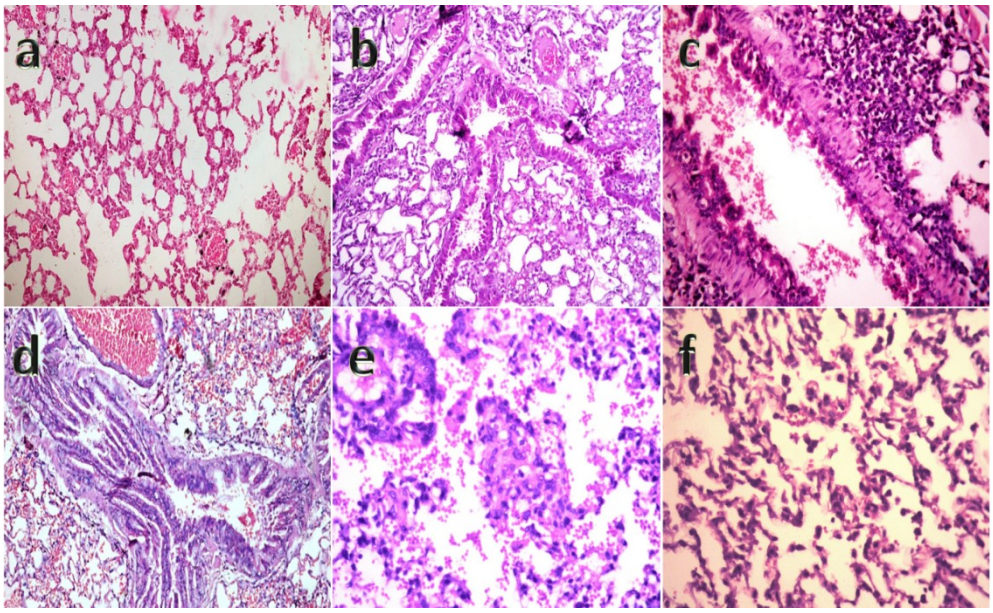

Fig. 1. (1a) Lung, mouse control revealing normal histological structure Lung, mouse intoxicated with benzo [a] pyerene At 3 months half dose (Fig 1 b) showing hyperplasia of the bronchiolar epithelium, emphysema in some pulmonary alveoli, other alveoli appeared atelectatic (H&E X200),At 6 months halfdose (Fig 1 c) showing hyperplasia of small round cells at the vicinity of pulmonary bronchioles (H&E X400),At 9 months halfdose (Fig 1 d) the bronchiolar epithelium revealing hyperplasia forming fronds like projection towards the lumen, At 9 months halfdose (Fig 1 e) one of the pulmonary bronchiole revealing a solid mass of proliferated cells in the pulmonary parenchyma more over proliferated bronchiolar epithelium in the lumen of the adjacent alveoli (H&E X400), At 9 months halfdose (Fig 1 f) proliferated bronchiolar epithelium in the lumen of the pulmonary alveoli in addition to macrophages and plasma cells also appeared in the lumen of the alveoli (H&E X200).

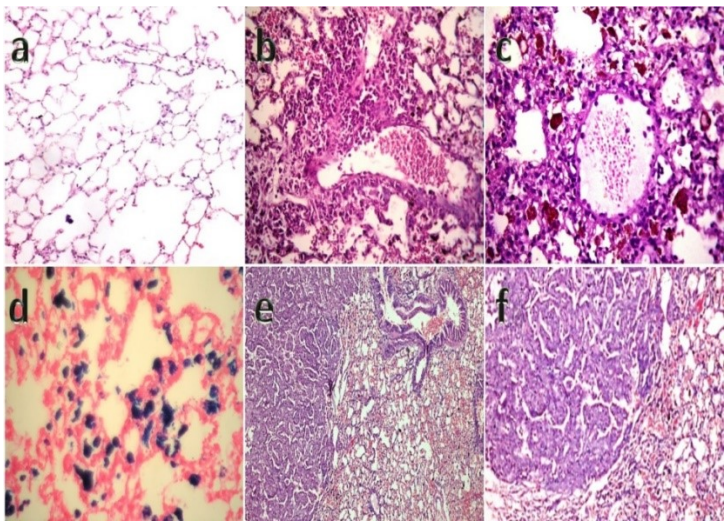

Fig. 2. (2a) lung mouse control showing normal histological structure, lung mouse intoxicated with benzo[a] pyerene At 3 months full dose (Fig 2 b) revealing widely dilated and engorged pulmonary blood vessels and perivascular hyperplasia of small rounded cells (H&E X400), At 6 months full dose (Fig 2 c) The pulmonary tissue demonstrating large macrophages and or multi nucleated syncytial giant cell dispersed in the pulmonary parenchyma containing golden yellow hemosiderin pigment (H&E X400),At 6 months full dose(Fig 2 d) demonstrating positive reaction of hemosiderin pigment stained blue with prussian blue pigment (Prussian blue X400), At 9 months full dose (Fig 2 e) The pulmonary tissue illustrating circumscribed tumor mass composed of proliferated bronchiolar epithelium (H&E X200).(Fig. 2f) higher magnification of the previous picture (tumor mass) (H&E X400)

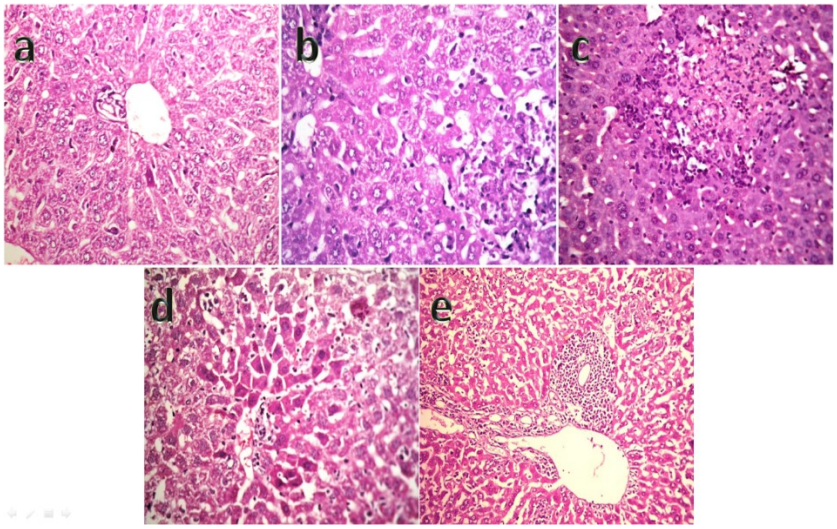

Fig. 3. (3a) liver of control mouse showing normal histological structure . Liver mouse intoxicated with benzo[a] pyerene At 3 months half dose (Fig. 3 b) the hepatic tissue showing focal circumscribed area of hepatocellular necrosis, some hepatocytes showing individual cell necrosis and frequent mitosis is also evident (H&E X400), At 6 months half dose (Fig. 3 c) the hepatic tissue showing circumscribed focal area of hepatocellular necrosis, which invaded by mononuclear cells, the adjacent hepatocytes showing numerous mitotic figures (H&E X200),At 9 months half dose (Fig. 3 d) The hepatic tissue illustrated hypertrophied hepatocytes, the hepatocytes are polygonal in shape together with multiple foci of hepatocellular alteration, mitotic figures are evident (H&E X400), At 9 months half dose (Fig. 3e) The portal area showed newly formed bile ductules which infiltrated by mononuclear cells (H&E X200).

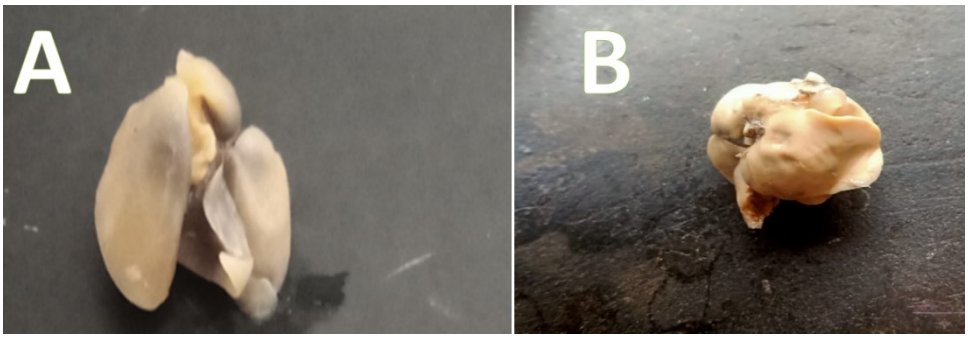

Fig.4. (4A) lung of a mouse intoxicated with benzo[a] pyerene at 9 months full dose showing nodule on the lung surface (Fig. 4B) liver of a mouse intoxicated with benzo[a] pyerene at 9 months full dose revealing foci of depression and others of elevation.

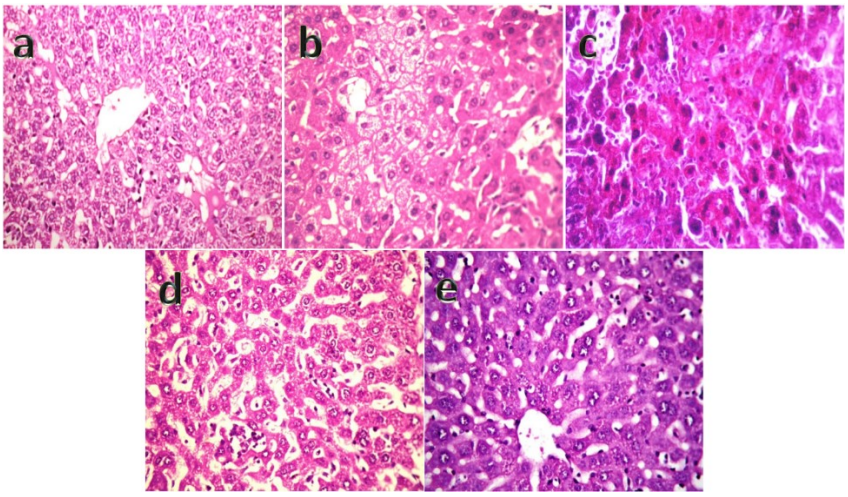

Fig. 5. (Fig 5a) Liver of control mouse showing nearly normal histological structure (Fig. 4a) liver mouse intoxicated with benzo [a] pyerene At 3 months full dose (Fig. 4 b) the hepatic tissue revealing multiple foci of hepatocellular alteration, some hepatocytes appeared hypertrophied and exhibited glycogen accumulation manifested by clearance of the cytoplasm (H&E X400), At 3 months full dose (Fig 4 c) hypertrophied hepatocytes by PAS stain showing glycogen accumulation inside the hepatocytes which stained scarlet red color (PAS X400), At 6 months full dose (Fig. 4d) the hepatic tissue revealing proliferated hepatocytes arranged in acinar pattern, moderate cellular and nuclear atypia, numerous mitotic figures the mitotic index was 4-6 per high power field are evident in the proliferated cells (H&E X400) , At 9 months full dose(Fig. 4e) the hypertrophied hepatocytes with extremely enlarged nuclei, marginated nuclear chromatin (H&E X400).

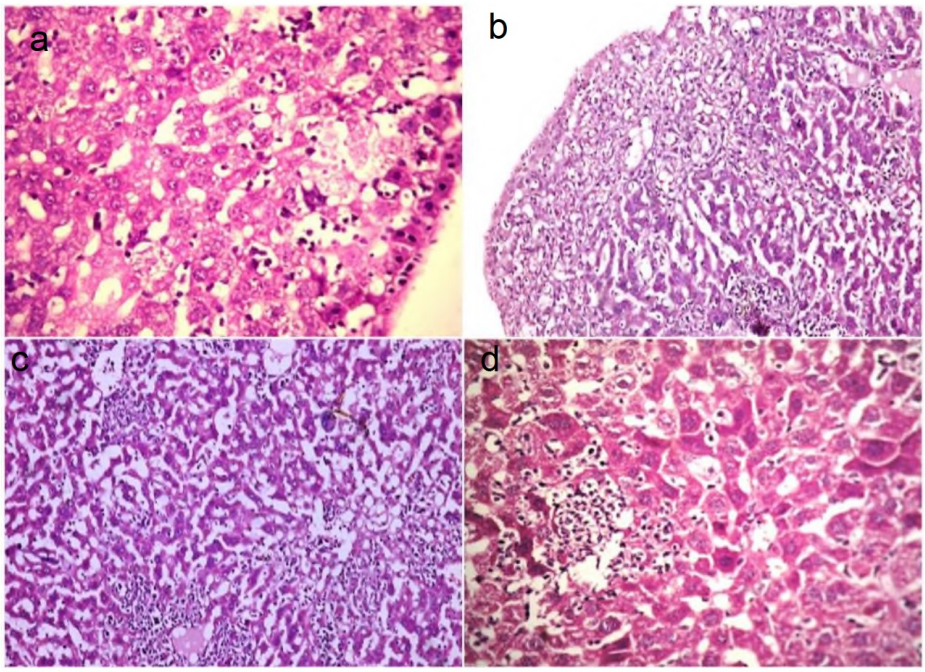

Fig.6. (6a) liver of mouse intoxicated with benzo [a] pyerene full dose at (6 months) showing interacytoplasmic micro vacuoles in the proliferated hepatocytes (H&E X400)(at 9 months) (Fig. 6b) The hepatic tissue illustrated hepatocellular carcinoma with multiple fat droplets in the cytoplasm of the neoplastic cells (H&E X200). (Fig. 6c) Hepatocellular carcinoma in which the neoplastic cells were arranged at variable configuration trabecular or acinar pattern and seprated by dilated hepatic sinusoids, sometimes hepatocytes coalesed and form multinucleatd syncytial giant cell (H&E X200) (Fig. 6d) The hepatocellular carcinoma cells are polygonal in shape with pleomorphic nuclei and multiple nucleoli (H&E X400)

References

1. IARC, Diesel and gasoline engine exhausts and some nitroarenes. IARC Monographs on the Evaluation of Carcinogenic Risks to Humans, 105, 1–703(2014)

2. Ramesh, A., Walker, S.A., Hood, D.B., Guillen, M.D., Schneider, H. and Weyand, E.H. Bioavailability and risk assessment of orally ingested polycyclic aromatic hydrocarbons (review). *Int. J. Toxicol.,* **23**, 301–333(2004).

3. Poirier, M.C. and Beland, F.A. DNA adduct measurements and tumor incidence during chronic carcinogen exposure in animal models: implications for DNA adduct-based human cancer risk assessment. *Chemical Research in Toxicology*, **32**, 103-115(2019)

4. Kévin, H., Elise, S., Anthony, L., Morgane, F., Isabelle, G., Cécile, H.T., Baharia, M., Samantha, A., Paule, B., Pierre, R., Maxime, J., Florence, H., Chris, O., Marie, T.L., Chantal, B., Odile, S., Huc, B. and Dominique, L.G. The environmental carcinogen benzo [a] pyerene induces a Warburg- like metabolic reprogramming dependent on NHE1 and associated with cell survival. *Scientific Reports*, **6**(1),30776(2016)

5. Bukowska, B., Mokra, K. and Michalowicz, J. Benzo[a]pyrene- Environmental Occurrence, Human Exposure, and Mechanism of Toxicity. *Int. J. Mol. Sci.,* **23** (11), 6348(2022).

6. Topinka, J. and Gori, G.B. Environmental PAH exposure and lung cancer. *Environmental Science and Pollution Research,* **27**(31), 38699-38705(2020).

7. Barnwal, P.A. and Vafa M. and Sultana, S. Benzo(a)pyrene induces lung toxicity and inflammation in mice: prevention by carvacrol human experimental toxicology. *Hum. Exp. Toxicol.,* **37**, 752-761(2018).

8. Fanali, Z., Franco-Belussi, L., Bonini-Domingos, C.R. and Oliveira, C., Effects of benzo[a]pyrene on the blood and liver of Physalaemus cuvieri and Leptodactylus fuscus (Anura:Leptodactylidae).*Environmental Pollution*, **237**, 93–102(2018).

9. Phillips, D.H. DNA adducts in human tissues: biomarkers of exposure to carcinogens in tobacco smoke. *Environmental and Molecular Mutagenesis,* **56**(1),1-8(2015).

10. Alexei, J., Likhachev, A., Dzamal, S.H., Beniashvili, R., Vladimir, J., Bykov, A., Pavel, P., Dikun, G., Margarita, L., Tyndyk, Y., Irina, V., Savochkina, H., Vladimir, B., Yermilov, H. and Mark, A.Z. Biomarkers for Individual Susceptibility to Carcinogenic Agents:Excretion and Carcinogenic Risk of Benzo[a]pyrene Metabolites *Environmental Health Perspectives,* **98**,211-214(1992).

11. Reitman, S. and Frankel, S. Colorimetric method for determination of serum AST and ALT. *Am. J. Clin. Pathol.,* **28**, 56-58(1957).

12. D S Chen, J L Sung, J C Sheu, M Y Lai, S W How, H C Hsu, C S Lee, T C Wei. Serum alpha-fetoprotein in the early stage of human hepatocellular carcinoma. *Gastroenterology,* **86**(6),1404-1409(1984).

13. Bancroft, J. and Gamble, A. Theory and practice of histological techniques, 6th edn. Churchill Livingstone, New York, London 2013; 165–175.

14. American College of Radiology. Liver Imaging Reporting and Data System 2018; https://www.acr.org/Clinical-Resources/Reporting-and-Data-Systems/LI-RADS.

15. SPSS 14. Statistical package for social science, SPSS for windows re-lease 14.0.0 12 Jun, 2006. Standard version, copyright SPSS Inc., 1989-2006, copyright (R) SPSS inc.m

16. Ching, E.W., Williane, H.L., Siupaul, K.S., Lihong, X.U., Zhang, Y., Richarbson, B.J. and Rudolf, S.S. DNA adducts formation and DNA strand breaks in Green Lipped Musssels (perma virridis) exposed to benzo a pyerene dose and time dependant relationship. *Marine Pollution Bulletin,* **42**(7), 603-610(2001).

17. Meuwissen, R. and Berns, A. Mouse model for human lung. *Gens and Development*, **19**, 643-664(2005).

18. Noack, A.T. and Winkelmann, F.T. The Clara Cell: "Third Reich eponym. *European Respiratory Journal,* **36**, 722-727(2010).

19. Ceteci, F., Semra, C., Emanuele, Z., Chitra, T., Matthias, B., Nefertiti, E., Ludger, F., Werner, S., Rajkumar, S. and Ulf , R.R. E-cadherin Controls Bronchiolar Progenitor Cell and Onset of Preneoplastic Lesion in Mice. *Neoplasia,* **14** (12), 1164-1177(2012).

20. Marzena, W.S., Mateusz, T.D., Ewa, S.J. and Jerzy, J. Proteolysis is the most fundamental property of malignancy and its inhibition may be used therapeutically. *Medicine,* **7**, 15-25(2018).

21. Kasala, E.R., Bodduluru, L.N., Barua, C.C., Sriram, C.S. and Gogoi, R. Benzo (a) Pyerene induced lung cancer: Role of dietary phytochemicals in chemoprevention. *Pharmacol. Rep.*, **67**, 996-1009(2015).

22. Panandiker, A., Maru, G.B. and Rao, K.V. Dose response effects of malachite green on free radical formation, lipid peroxidation and DNA damage in hamster embryo cells and their modulation by antioxidants. *Carcinogenesis,* **15**, 2445-2448(1994).

23. Sikkim, H. and Mulee, B. Lipid peroxidation and antioxidant enzymes in the blood of rats treated with benzo [a] pyerene. *Chem. Biol. Interact.,* **127**,139-150(2000).

24. Kim, H.S., Kwack, S.J. and Lee, B.M. Lipid peroxidation, antioxidant enzymes, and benzo [a] pyerene- quinones in the blood of rats treated with benzo [a] pyerene. *Chem. Biol. Interact.,* **127**,139-150(2000).

25. Deng, C.H., Dang, F., Gao, J., Zhao, H., Qi, S.H. and Gao, M. Acute benzo[a]pyrene treatment causes diferent antioxidant response and DNA damage in liver, lung, brain, stomach and kidney. *Heliyon,* **4**(11), e00898 (2018).

26. Tahir, M., Rehman, M.U., Lateef, A., Quaiyoom, A., Khan, R., Hamiza, O.O., Ali, F., Hasan, S.K. and Sultana, S. Diosmin abrogates chemically induced hepatocarcinogeesis via alleviation of oxidative stress, hyperproliferative and inflammatory markers in murine model. *Toxicol. Lett.,* **220**, 205-218(2013).

27. Cuccurullo, V. and Mansi, L. AJCC Cancer Staging Handbook: from the AJCC Cancer Staging Manual

(7th edition). *European Journal of Nuclear Medicine and Molecular Imaging*, **38**, 408-408(2010).

28. Buendia, M.A. and Neuveut, C. Hepatocellular carcinoma .*Cold Spring Harbor Perspectives in Medicine*, **5**(2), Article ID: ao21444(2015).

29. Gao, F., Zhu, H.K. and Zhu ,Y.B. Predictive value of tumor markers in patients with recurrent hepatocellular carcinoma in different vascular invasion pattern. *Elsevier Pancreatic Disease*, **15**, 371-377(2016).

30. Xueyi, L.I., Shenyuan, H.E., Chunxia, G.A., Hong, D., Yongfeng, L. and Cuiqin, L. Iso orientin attenuates benzo [a] pyerene induced liver injury by inhibiting autophagy and pyroptosis in vitro and vivo. *Scientific Reports*, **6**, 841-861(2019).

31. Zhang, Y., Fan, Y., Gao, J., Xu, W., Xu, Z., Liu, Y. and Tao, L. A new 24-membered macrolide shows insecticidal activity against Pieris rapae potentially through induction of programmed cell death. *Food and Agricultural Immunology,* **30**, 727–742(2019).

32. Gorria, M., Tekpli, X., Rissel, M., Sergent, O., Huc, L., Landvik, N. and Lagadicgossmann, D.A. New lactoferrin-and iron-dependent lysosomal death pathway is induced by benzo[a]pyrene in hepatic epithelial cells. *Toxicology and Applied Pharmacology*, **228**,212–224(2008).

33. Yuan, L., Liu, J., Deng, H. and Gao, C. Benzo[a]pyrene induces autophagic and pyroptotic death simultaneously in HL-7702 human control liver cells. *Journal of Agricultural and Food Chemistry,* **65**, 9763–9773(2017).

34. Qamar, W., Khan, A.Q., Khan, R., Lateef, A., Tahir, M., Rehman, M.U., Ali, F. and Sultana, S. Benzo (a) Pyrene- induced pulmonary inflammation, edema, surfactant dysfunction, and injuries in rats: alleviation by farnesol. *Exp. Lung Res.,* **38**, 19-27(2012).

35. Hardonnière, K., Huc, L., Podechard, N., Fernier, M., Tekpli, X., Gallai, I. and Lc, G.D. Benzo[a]pyrene-induced nitric oxide production acts as a survival signal targeting mitochondrial membrane potential. *Toxicology in Vitro.* **29**, 1597–1608(2015).

36. Manabu, M., Yusuke, A.S., Kaori, E., Shigeyuki, U., Toshiyuki, M.K., Sachiko, Y. and Makoto, M. The aryl hydrocarbon receptor activator benzo [a] pyerene enhances vitamin D3 catabolism in macrophages. *Toxicol. Sci.,* **109** (1), 50-58(2009).

37. Haschecck, W.M. and Rousseaux, C.G. Fundmentals of Toxicologic.Pathology. 1998;Academic Press, San Diego, London. Newyork, BOSTON, Sydney, Tokyo, Toronto

38. Butterworth, B.E., Templin, M.V., Constan, A.A., Sprankle, C.S., Wong, B.A., Pluta, L.J., Everitt, J.I. and Recio, L. Long- term mutagenicity studies with chloroform and dimethyl nitrosamine in female Ia CI Transgenic B6 C3F. sub (1) mice. *Environ. Mol. Mutag.,* **31** (3),248-256(1998).

39. Fatma, M.D. and Amany, E.Y. Biochemical and pathological studies of the effect of A chemical Carcinogen Dimethyl nitrosamine (DMN) in mice. *Egyptian Journal OF Comparative Pathology & Clinical Pathology*, **15**, 29- 56(2002).

40. Zachary, J.F. and Donald, M. Pathologic Basis of Veterinary Disease Fifth Edition 2012; Elsiever.

41. Rubin, H. Synergistic mechanisms in carcinogenesis by polycyclic aromatic hydrocarbons and by tobacco smoke: a bio-historical perspective with updates. *Carcinogenesis,* **2**(22),1903–1930(2001).

42. Qian, C., Fang, Y., Chen, H., Yun, C., Hui, P. and Ke-Jian, W. Benzo [a] Pyerene (BaP) exposure generates persistent reactive oxygen species (ROS) to inhibit the NF-Kb pathway in medaka (Oryzias melastigma). *Environ Pollut*., **251**,502-509(2019).

التغيرات المرضية فى الرئة والكبد فى ذكور الفئران المسممة بالبنزو[أ]بيرين: دراسة تعتمد على الزمن

دعاء احمد حسن[1] فاطمة محمود درويش[1] ايمان بكر محمد[2]

[1] قسم الباثولوجى - معهد بحوث الصحة الحيوانية - الدقى – مصر.
[2] قسم الباثولوجى - كلية الطب البيطرى - جامعة القاهرة – مصر.

الخلاصة :

هدفت هذه الدراسة إلى دراسة التغيرات المرضية في الرئة والكبد لدى الفئران المعرضة لجرعات مختلفة من البنزو[أ]بيرين على مدى فترات مختلفة. تم تقسيم تسعين فأرا ناضجا إلى ثلاث مجموعات: مجموعة ضابطة سلبية، تم حقن مجموعة بجرعة وحيدة قدرها 50 ملغم/كغم من وزن الجسم من البنزو[أ]بيرين ، ومجموعة تم حقنها بجرعة واحدة قدرها 100 ملغم/كغم من وزن الجسم من البنزو[أ]بيرين وأجريت التجربة لمدة 9 أشهر. تم ذبح عشرة فئران من كل مجموعة عند 3، 6، و 9 أشهر. تم جمع عينات المصل لإجراء الاختبارات البيوكيميائية (وظائف الكبد ومستويات بروتين ألفا). تم إجراء فحوصات ما بعد الوفاة، وتم جمع عينات من أنسجة الرئة والكبد لتحليلها النسيجي المرضي. أظهرت نتائج الاختبارات الكيموحيوية وجود زيادة في مستويات إنزيم ناقلة أمين الألانين (ALT) وناقلة أمين الأسبارتات (AST) والبروتين الجنيني ألفا. أظهر الفحص النسيجي المرضي لأنسجة الرئة تكاثرًا مفرط التنسج في ظهارة القصيبات، مع حدوث تغيرات أكثر وضوحًا في مجموعات الجرعة الكاملة عند 6 و9 أشهر. بعد 9 أشهر من العلاج بالجرعة الكاملة، تم اكتشاف كتلة ورم محددة جيدًا في الكبد، لوحظت تغيرات خلوية عند 3 أشهر لكل من الجرعات النصفية والكاملة من البنزو[أ]بيرين ، وتتطور إلى تغيرات خبيثة عند 6 أشهر وتؤدي في النهاية إلى تطور سرطان غدي خلوي كبدي عند 9 أشهر.

الكلمات الدالة: البنزو[أ]بيرين، الرئة، الكبد، التشريح المرضي.